Free Radical Biology and Medicine 80 (2015) 93–100

Contents lists available at ScienceDirect

Free Radical Biology and Medicine

journal homepage: www.elsevier.com/locate/freeradbiomed

Original Contribution

Insights into the mechanism of the reaction between hydrogen sulfide and peroxynitrite

Ernesto Cuevasanta [a,b], Ari Zeida [c], Sebastián Carballal [b,d], Rudolf Wedmann [e], Uriel N. Morzan [c], Madia Trujillo [b,d], Rafael Radi [b,d], Darío A. Estrin [c], Milos R. Filipovic [e,*], Beatriz Alvarez [a,b,**]

[a] Laboratorio de Enzimología, Facultad de Ciencias, Universidad de la República, 11400 Montevideo, Uruguay
[b] Center for Free Radical and Biomedical Research, Universidad de la República, 11800 Montevideo, Uruguay
[c] Departamento de Química Inorgánica, Analítica, y Química-Física and INQUIMAE-CONICET, Facultad de Ciencias Exactas y Naturales, Universidad de Buenos Aires, C1428EHA Buenos Aires, Argentina
[d] Departamento de Bioquímica, Facultad de Medicina, Universidad de la República, 11800 Montevideo, Uruguay
[e] Department of Chemistry and Pharmacy, University of Erlangen–Nuremberg, 91058 Erlangen, Germany

ARTICLE INFO

Article history:
Received 14 October 2014
Received in revised form
12 December 2014
Accepted 18 December 2014
Available online 30 December 2014

Keywords:
Hydrogen sulfide
Peroxynitrite
Kinetics
Persulfides
Free radicals

ABSTRACT

Hydrogen sulfide and peroxynitrite are endogenously generated molecules that participate in biologically relevant pathways. A revision of the kinetic features of the reaction between peroxynitrite and hydrogen sulfide revealed a complex process. The rate constant of peroxynitrite decay, $(6.65 \pm 0.08) \times 10^3\ M^{-1}\ s^{-1}$ in 0.05 M sodium phosphate buffer (pH 7.4, 37 °C), was affected by the concentration of buffer. Theoretical modeling suggested that, as in the case of thiols, the reaction is initiated by the nucleophilic attack of HS^- on the peroxide group of ONOOH by a typical bimolecular nucleophilic substitution, yielding HSOH and NO_2^-. In contrast to thiols, the reaction then proceeds to the formation of distinct products that absorb near 408 nm. Experiments in the presence of scavengers and carbon dioxide showed that free radicals are unlikely to be involved in the formation of these products. The results are consistent with product formation involving the reactive intermediate HSSH and its fast reaction with a second peroxynitrite molecule. Mass spectrometry and UV–Vis absorption spectra predictions suggest that at least one of the products is $HSNO_2$ or its isomer HSONO.

Hydrogen sulfide[1] is being considered a new signaling molecule in mammals after the discovery of its formation in vivo and its modulatory effects. It is produced in tissues of mammals through the activity of cystathionine β-synthase and cystathionine γ-lyase, two pyridoxal phosphate-dependent enzymes, and probably also of mercaptopyruvate *S*-transferase [1]. Although the concentrations of hydrogen sulfide measured in vivo are not high—just tens of nanomolar [2]—several effects, including neuromodulator and vasodilator properties [3,4], have been described in research model systems, and the administration of hydrogen sulfide or the modulation of its production are of possible pharmacological interest

In the context of efforts to rationalize the potential of hydrogen sulfide to act as a scavenger of biological oxidants, the reaction with peroxynitrite[2], the product of the fast recombination of nitric oxide with superoxide radicals, drew the attention of two research groups [5,6]. Two independent determinations of the rate constant reached slightly different results. Carballal et al. [5] reported a value of $(4.8 \pm 1.4) \times 10^3\ M^{-1}\ s^{-1}$ and Filipovic et al. [6] reported a value of $(8 \pm 2) \times 10^3\ M^{-1}\ s^{-1}$, both at 37 °C and pH 7.4. Carballal et al. proposed a reaction mechanism analogous to the classic one proposed for thiols with peroxynitrite [7–13]. Like in the case of low- and high-molecular-weight thiols, the proposed reaction mechanism involved the formation of a sulfenic acid-like product (HSOH) after the attack of HS^- on ONOOH. This intermediate would react

* Corresponding author at: Department of Chemistry and Pharmacy, Friedrich-Alexander University of Erlangen-Nuremberg, 91058 Erlangen, Germany. Tel.: +49 9131 852 7345.
** Corresponding author at: Laboratorio de Enzimología, Facultad de Ciencias, Universidad de la República, 11400 Montevideo, Uruguay. Fax: +598 2525 0749.
E-mail addresses: milos.filipovic@fau.de (M.R. Filipovic), beatriz.alvarez@fcien.edu.uy (B. Alvarez).

[1] The term "hydrogen sulfide" is used in this text for the mixture of H_2S and HS^- present in aqueous solution according to the working pH, unless otherwise specified. The IUPAC-recommended names are sulfane and hydrogen sulfide for H_2S and sulfanide and hydrogen(sulfide)(1−) for hydrosulfide anion, HS^-.

[2] "Peroxynitrite" is used to refer to the species in equilibrium, $ONOO^-$ and ONOOH. The IUPAC-recommended names are oxoperoxonitrate(1−) and hydrogen oxoperoxonitrate, respectively.

http://dx.doi.org/10.1016/j.freeradbiomed.2014.12.017
0891-5849/

with a new HS^- molecule to produce HSSH. Nevertheless, Filipovic et al. noticed the formation of an unexpected yellow product. The stability of this new product seemed to be low in the presence of oxygen. In addition, mass spectrometry results suggested the formation of $HSNO_2$ or its isomers. Another set of plausible reaction mechanisms was proposed, including concerted reactions and radical processes.

The two groups joined efforts to better understand the puzzling reaction between hydrogen sulfide and peroxynitrite, and this work provides new clues for the elucidation of its mechanism.

1. Materials and methods

1.1. Reagents and solutions

$Na_2S \cdot 9H_2O$ of high purity was purchased from J.T. Baker. Peroxynitrite was synthesized as previously described [5,14], diluted in 2 mM NaOH, and quantified by measuring absorbance at 302 nm ($\varepsilon_{302\ nm} = 1670\ M^{-1}\ cm^{-1}$) [15]. Phosphate and formate buffers were of high quality. The use of sodium hydroxide was avoided in the preparation of phosphate buffers. When sodium hydrogen carbonate was added, the final pH was adjusted to the desired value. DMPO[3], desferrioxamine, mannitol, potassium peroxymonosulfate, and cysteine stocks were prepared in ultrapure water. Sodium hypochlorite stock solution was diluted in 2 mM NaOH and measured at 292 nm. Hydrogen peroxide was diluted in ultrapure water and quantified at 240 nm. Tetranitromethane stock was prepared in phosphate buffer. H_2S_2 was synthesized following a previously reported protocol [16].

1.2. Kinetic measurements and UV–Vis spectral characterization of products

Kinetic measurements were performed in stopped-flow instruments using single-wavelength or photodiode array detectors (Applied Photophysics SX20 and μSFM-20 Bio-Logic stopped-flow module equipped with a J&M TIDAS high-speed diode array spectrometer with combined deuterium and tungsten lamps). Anaerobic conditions were achieved by displacing O_2 from vials and solutions with N_2 and flushing instruments with N_2-saturated water.

1.3. Mass spectrometry characterization

Reaction was performed in 20 mM ammonium formate buffer (pH 8.0) with or without dilution in acetonitrile and injected at −20 or +4 °C, respectively, using cryo-mass electron spray ionization (ESI). Spectra were recorded on an ultra-high-resolution ESI–time-of-flight (TOF) maXis mass spectrometer (Bruker Daltonics) and processed in data analysis software provided by the manufacturer.

1.4. Computational methods

1.4.1. Isolated species

To obtain information about the potential energy surface and the mechanism of the reaction under investigation, and to perform UV–Vis absorption spectra predictions, we performed several electronic structure calculations using the Gaussian 03 program [17]. The structures of the reactant complex (HS^-/ONOOH), product complex ($HSOH/NO_2^-$), and transition state (TS) of the first step of the reaction along with possible prospective intermediates were optimized both in vacuo and in the presence of up to four water molecules at different levels of theory: density functional theory (DFT) using the *PBE* functional and *MP2*, employing a double-zeta plus polarization (*dzvp*) Gaussian basis set [18]. Frequency calculations were performed in all cases. Intrinsic reaction coordinate and time-dependent DFT (TD-DFT) calculations were performed at the *PBE/dzvp* level of theory.

1.4.2. Aqueous solution absorption spectra prediction

This study was carried out using an all-electron Gaussian basis set density functional code developed by Nitsche et al. [19]. This code was interfaced with an Amber classical force field, to carry out hybrid quantum mechanics–molecular mechanics (QM–MM) simulations. Absorption spectra were calculated from an average of an ensemble of instantaneous configurations obtained from a QM–MM Born-Oppenheimer 50-ps molecular dynamics, which combined DFT at the *PBE/dzvp* level and the TIP3P force field to describe the H_2O solvent molecules. A set of configurations extracted from these QM–MM trajectories were employed to perform the real-time TD-DFT level, using exactly the same *PBE/TIP3P* hamiltonian as the one adopted to perform the molecular dynamics. This methodology has proven to yield reliable predictions of absorption properties of molecules in solution or in complex environments [20].

1.5. Simulations and data analysis

Kinetic data were analyzed and fitted using the Pro-Data Viewer software (Applied Photophysics), Bio-Kine32 software (Bio-Logic), or Origin 6.1. Kinetic simulations were performed with GEPASI [21].

2. Results and discussion

2.1. Rate constant of peroxynitrite decay at 302 nm

In the previous reports, Carballal et al. had used NaHS, whereas Filipovic et al. had used Na_2S [5,6]. Thus, the difference in rate constants determined by both groups was initially thought to be related to the hydrogen sulfide source (NaHS vs Na_2S), because NaHS stocks can contain significant amounts of impurities [22]. However, new determinations of the rate constant for peroxynitrite consumption using Na_2S led to results quite similar to the previous ones using NaHS, consistent with the fact that the NaHS used before had been titrated [5]. Another difference in the procedures was the buffer concentration (potassium phosphate 0.3 M used by Filipovic et al. vs 0.1 M used by Carballal et al.). As observed in Fig. 1, the second-order rate constant was $(9.1 \pm 0.3) \times 10^3\ M^{-1}\ s^{-1}$ (37 °C, pH 7.4) with 0.3 M potassium phosphate buffer, but the rate constant was $(6.65 \pm 0.08) \times 10^3\ M^{-1}\ s^{-1}$ with 0.05 M buffer. Also, the decay of peroxynitrite alone was faster in the high-concentration buffer. These observations can be explained by the effect of buffer concentration—not ionic strength—on the pK_a of peroxynitrous acid according to previous reports [23,24]. It has been shown that the higher the phosphate concentration, the higher the pK_a of peroxynitrous acid. We can argue that when the pK_a increases, a higher amount of peroxynitrous acid (ONOOH; the reactive species toward HS^-) is present in solution at pH 7.4 and thus its spontaneous decay as well as its consumption by HS^- is faster.

From the value of $(6.65 \pm 0.08) \times 10^3\ M^{-1}\ s^{-1}$ at pH 7.4 (37 °C, 0.05 M sodium phosphate buffer) we can extrapolate a pH-independent rate constant of $(5.6 \pm 0.6) \times 10^4\ M^{-1}\ s^{-1}$ assuming pK_a of 6.7 and 7.0 for peroxynitrous acid and hydrogen sulfide, respectively [23,25]. Compared to the rate constants of low-molecular-weight thiolates, we can conclude that HS^- has a slightly lower nucleophilic character than aliphatic thiolates [5], probably because of the absence of the substituent methylene group and its inductive effect.

[3] *Abbreviations used:* DMPO, 5,5-dimethyl-1-pyrroline *N*-oxide; DTPA, diethylenetriaminepentaacetic acid; TS, transition state; QM–MM, quantum mechanics–molecular mechanics; DFT, density functional theory; TD-DFT, time-dependent DFT.

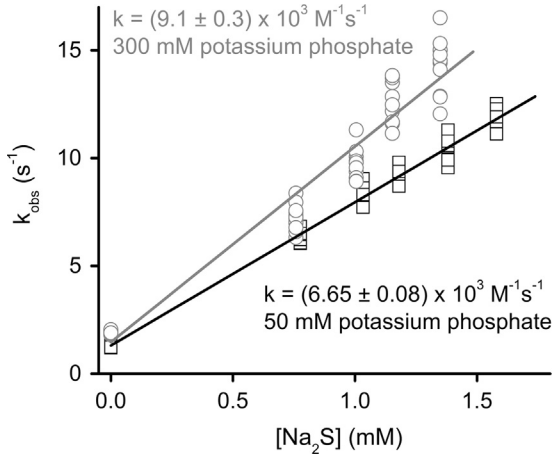

Fig. 1. Dependence of the rate constant on buffer concentration. The decay of peroxynitrite (54 μM) was followed by measuring the absorbance at 302 nm in the presence of increasing concentrations of sodium sulfide at 37 °C and pH 7.4. The k_{obs} was determined by fits to single exponential functions. Gray points were obtained using 0.30 M potassium phosphate buffer with 0.1 mM DTPA and black points using the same buffer diluted to 0.05 M with 0.1 mM DTPA.

2.2. Kinetics of product formation at 408 nm

The absorbance increase at 408 nm was complex. A lag could be detected in the first milliseconds. Then, a relatively large increase in absorbance occurred up to ~0.2 s and was followed by a slower increase at higher time points that could also be detected at 302 nm (Fig. 2A). At even higher time points, after 5 s (not shown), decay of the absorbance at 408 nm was observed, in agreement with the yellow product being unstable under aerobic conditions. Kinetic traces at 408 nm lacking the first 10 ms were fit to double-exponential functions. The k_{obs} of the first phase (the phase with the largest amplitude) were lower than the k_{obs} obtained from kinetic traces at 302 nm (Fig. 2B). Under anaerobic conditions, where the stability of the yellow product is higher, phenomena similar to those shown in Fig. 2 were observed (not shown). One possible explanation for these observations is that the formation of the products that absorb at 408 nm does not occur in a one-step process but that it occurs through consecutive reactions and involves intermediates.

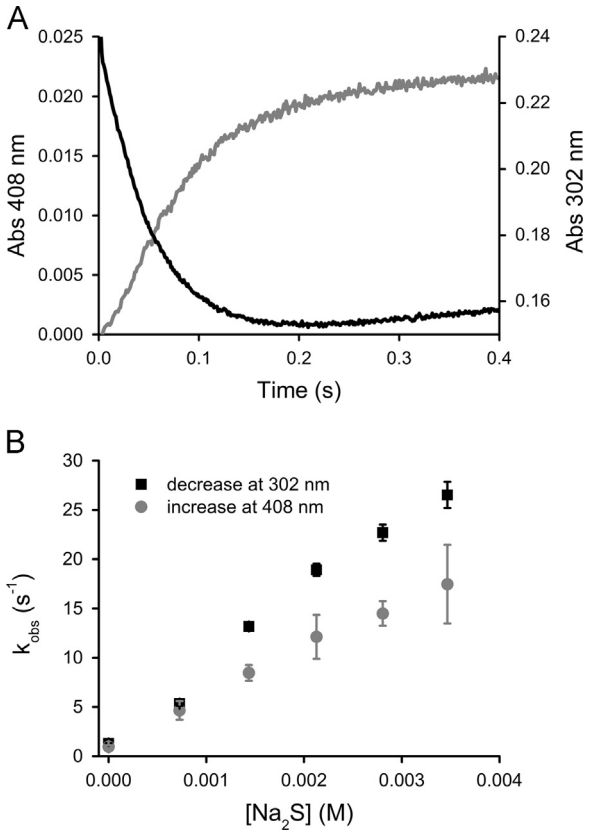

Fig. 2. Reaction between hydrogen sulfide and peroxynitrite at 302 and 408 nm. (A) Representative kinetic trace at 302 (black) and 408 nm (gray) obtained with 2.1 mM Na_2S and 0.2 mM peroxynitrite in 0.1 M potassium phosphate with 0.1 mM DTPA, pH 7.3, at 37 °C. (B) The k_{obs} was determined by fits to single-exponential plus straight-line functions at 302 nm (black points) or double-exponential functions at 408 nm omitting the first 10 ms (gray points).

2.3. Comparison with the reaction between peroxynitrite and cysteine

To clarify whether an analogous yellow product is formed in the presence of thiols instead of hydrogen sulfide, we obtained time-resolved UV–Vis spectra of mixtures of peroxynitrite with cysteine. There were no increases in absorbance at ~400 nm, only the decay of the peroxynitrite absorption could be detected (Fig. 3).

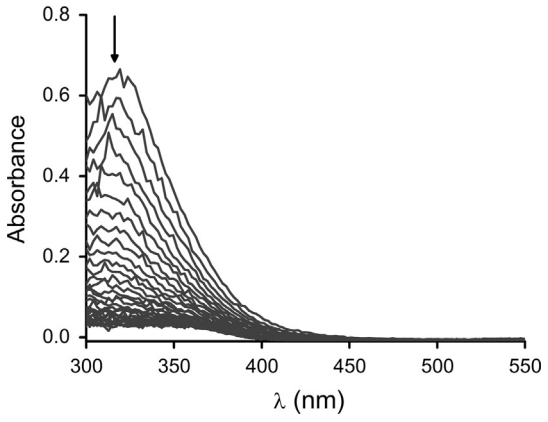

Fig. 3. Reaction of cysteine with peroxynitrite. Cysteine (10 mM) was mixed with peroxynitrite (1 mM) in 0.1 M potassium phosphate with 0.1 mM DTPA, pH 7.2, at 37 °C and UV–Vis spectra were recorded for 0.1 s, every 0.003 s. The arrow indicates the decay of the absorbance of peroxynitrite. No further changes were detected up to 200 s (not shown).

2.4. Theoretical modeling of the reaction between hydrogen sulfide and peroxynitrite

To shed light on the first step of the process, theoretical modeling of the attack of HS^- on ONOOH was performed. Peroxynitrite has been the subject of several theoretical studies, which aided in the understanding of its structural and electronic properties [26–28]. Nevertheless, this is the first attempt to study its reactivity against hydrogen sulfide. A free energy scheme of the first step of the reaction is shown in Fig. 4 (for a comparison of free energy determinations with different methodologies see Supplementary Table S1). The profile shows an exergonic process with $\Delta G_{rxn} \approx -50$ kcal/mol and $\Delta G^{\ddagger} = 10.8$ kcal/mol. This activation free energy is consistent with the rate constant determined and is also in good agreement with previous experimental and theoretical values for the reaction of cysteine with peroxynitrite [12]. Furthermore, these calculations correlate with experiments performed by Filipovic et al. for the temperature dependence of the apparent rate constant at pH 7.4 of the reaction between hydrogen sulfide and peroxynitrite, from which an apparent $\Delta G^{\ddagger}$ value of 11.1 kcal/mol can be estimated at 25 °C [6].

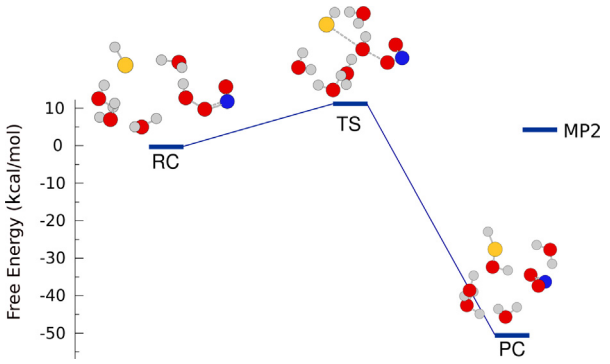

Fig. 4. Free energy scheme of the first step of the reaction between hydrogen sulfide and peroxynitrite. Reactant complex (RC) (HS^-/ONOOH), transition state (TS), and product complex (PC) (HSOH/NO_2^-) free energy values (kcal/mol) and their respective structures. Values and geometries depicted were obtained from geometry optimizations and frequency calculations at the *MP2/dzvp* level of theory including four water molecules.

The observed mechanism is in agreement with a typical bimolecular nucleophilic substitution (S_N2), in which the sulfur acts as the nucleophile [29], yielding HSOH and NO_2^- as products. The TS is characterized by the alignment of the S atom with both peroxide O atoms, an increase in the O–O peroxide distance, and the concomitant subtle charge reorganization (see coordinates and Mulliken populations in Supplementary Tables S2 and S3) [12]. It is worth noting that the same mechanism was observed with or without the inclusion of water molecules for both DFT and *MP2* calculations. Further evidence of a nucleophilic substitution mechanism is the fact that, for two peroxides studied (hydrogen peroxide and peroxynitrous acid) [5], the rate constants increase with the acidity of the conjugate acid of the leaving group (water and nitrous acid, pK_a 15.7 and 3.15, respectively).

2.5. Possible intermediates involved in the reaction between peroxynitrite and hydrogen sulfide

It was first hypothesized that free radicals could be involved in the formation of the yellow product. However, the addition to the reaction mixture of CO_2 (25 mM $NaHCO_3$), which reacts fast ($4.6 \times 10^4\ M^{-1}\ s^{-1}$, pH 7.4, 37 °C) [30] with peroxynitrite yielding carbonate and nitrogen dioxide radicals, did not increase but rather inhibited the amount of product formed (Fig. 5A and B). In addition, we tried mannitol (5 mM) as a $^{\bullet}OH$ scavenger, desferrioxamine (5 mM) as a $^{\bullet}OH$ and $^{\bullet}NO_2$ scavenger [31], and DMPO (88 mM), which is able to trap thiyl radicals and presumably $HS^{\bullet}$. The use of these radical trapping molecules did not produce changes in the yield of the reaction (Supplementary Figs. S1A, S1B, S1C, S2A, and S2B), ruling out the participation of free radicals.

We also tested other oxidants (hydrogen peroxide, peroxymonosulfate, hypochlorous acid, and tetranitromethane), looking for the formation of the same yellow product upon mixing with hydrogen sulfide, but we did not find any evidence for its formation (Fig. 6A, B, C, and D).

Hypothesizing that nitrite—which is present in peroxynitrite reaction mixtures—was necessary for the formation of the yellow product, we prepared alternative mixtures that contained nitrite. As reported previously, the reaction of hydrogen sulfide with nitrite is extremely slow at neutral pH [32,33], and no product is expected to be formed in short time periods. Under acidic conditions a reaction occurs but the product absorbs at 370 nm [34]. Time-resolved spectra of mixtures of oxidants and hydrogen sulfide in the presence of nitrite were evaluated. The mixture of hydrogen sulfide (5 mM) with peroxymonosulfate (0.5 mM) in the presence of 5 mM nitrite showed an absorbance increase with a maximum at ~390 nm (Fig. 7A),

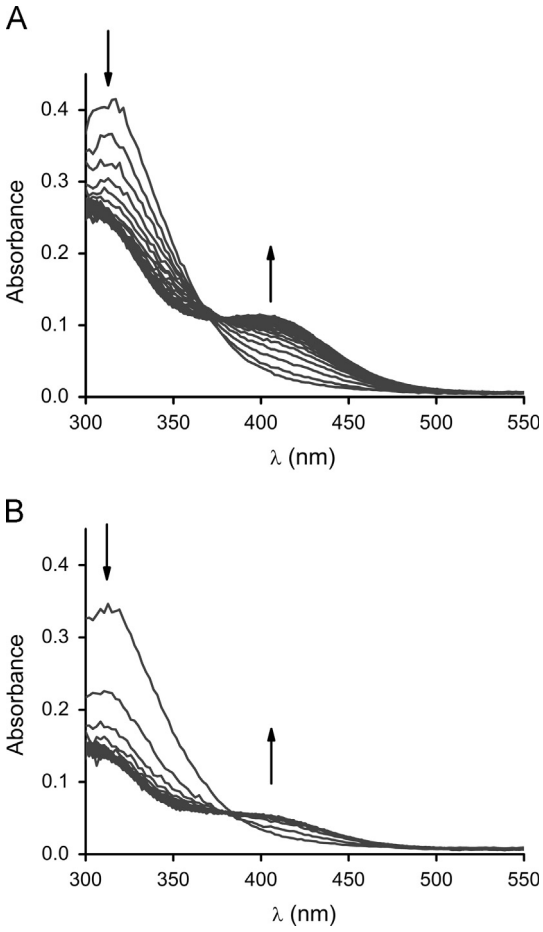

Fig. 5. Effect of CO_2 in the reaction of hydrogen sulfide with peroxynitrite. (A) Time-resolved spectra using 4.96 mM Na_2S and 0.5 mM peroxynitrite in 0.1 M potassium phosphate and 0.1 mM DTPA, pH 7.3, at 37 °C. Spectral changes were followed over 0.5 s, every 0.012 s. (B) Idem (A), with 25 mM $NaHCO_3$.

different from that observed under identical conditions but using peroxynitrite as oxidant. From these experiments, a second order rate constant of $(16.3 \pm 0.8) \times 10^3\ M^{-1}s^{-1}$ (pH 7.4, 37 °C) could be estimated for the reaction of hydrogen sulfide with peroxymonosulfate, in accordance with reported values [35].

In addition, the presence of nitrite while hydrogen sulfide reacted with peroxynitrite neither affected the yield of the yellow compound nor produced changes in the kinetics compared with hydrogen sulfide and peroxynitrite alone (Fig. 7B in comparison to Fig. 5A). Taken together, these results rule out the involvement of nitrite in the formation of the yellow product.

Finally, when peroxynitrite was present in excess, the amount of yellow product formed increased, suggesting the involvement of a second peroxynitrite molecule in the process (Fig. 8).

Thus, our hypothesis is that a nonradical reactive intermediate formed from the reaction of peroxynitrite with hydrogen sulfide reacts with peroxynitrite yielding the yellow product. One reaction sequence consistent with the results obtained is the following:

$$HS^- + ONOOH \rightarrow HSOH + NO_2^- \quad (1)$$

$$HSOH + HS^- \rightarrow HSSH/HSS^- + H_2O/OH^- \quad (2)$$

$$HSSH/HSS^- + ONOOH/ONOO^- \rightarrow \text{yellow compound} \quad (3)$$

To prove the feasibility of this reaction sequence, we performed computer-assisted kinetic simulations with rate constants of 6.65×10^3, 1×10^6, and $3 \times 10^4\ M^{-1}\ s^{-1}$ for the first, second, and third steps. The value assigned to the rate constant of the second step is

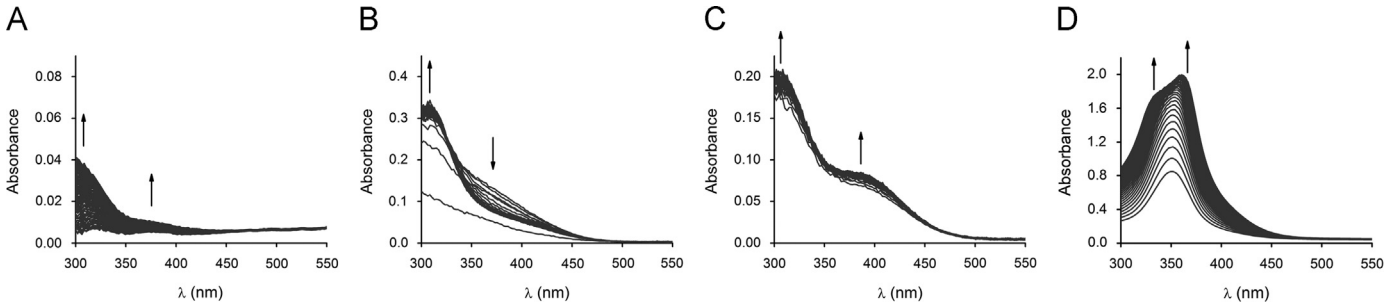

Fig. 6. Spectral characterization of hydrogen sulfide oxidation by hydrogen peroxide, peroxymonosulfate, hypochlorous acid, and tetranitromethane. Time-resolved UV–Vis spectra: (A) 4.96 mM Na_2S and 0.5 mM H_2O_2 in 0.1 M potassium phosphate and 0.1 mM DTPA, pH 7.3, at 37 °C. Spectra were recorded for 60 s, every 0.6 s. (B) 4.96 mM Na_2S and 0.5 mM peroxymonosulfate in 0.1 M potassium phosphate and 0.1 mM DTPA, pH 7.3, at 37 °C. Spectra were recorded for 0.5 s, every 0.012 s. (C) 4.96 mM Na_2S and 0.5 mM sodium hypochlorite in 0.1 M potassium phosphate and 0.1 mM DTPA, pH 7.3, at 37 °C. Spectra were recorded for 0.5 s, every 0.012 s. (D) 0.06 mM Na_2S and 0.06 mM tetranitromethane in 10 mM potassium phosphate buffer, pH 7.4, at 25 °C. Spectra were recorded for 0.4 s, every 0.012 s.

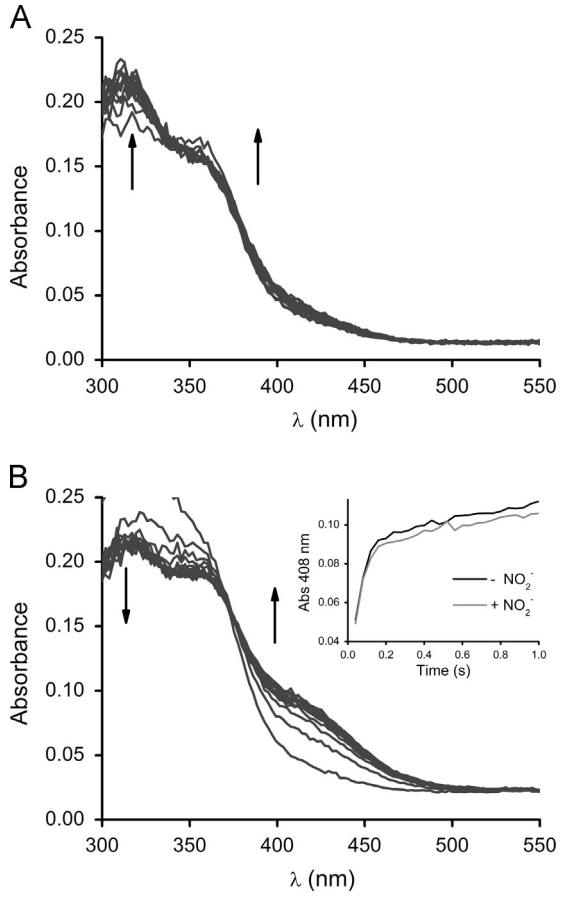

Fig. 7. Time-resolved spectra for the reaction of hydrogen sulfide with oxidizing mixtures including nitrite. Time-resolved spectra were recorded for 0.52 s, every 0.04 s, in 0.1 M potassium phosphate with 0.1 mM DTPA, pH 7.4 at 37 °C. (A) 5 mM Na_2S, 0.5 mM peroxymonosulfate, and 5 mM NO_2^-. (B) 5 mM Na_2S, 5.0 mM NO_2^-, and 0.5 mM peroxynitrite, to be compared with Fig. 5A. Inset: kinetic traces of absorbance at 408 nm obtained in the presence or absence of added NO_2^-.

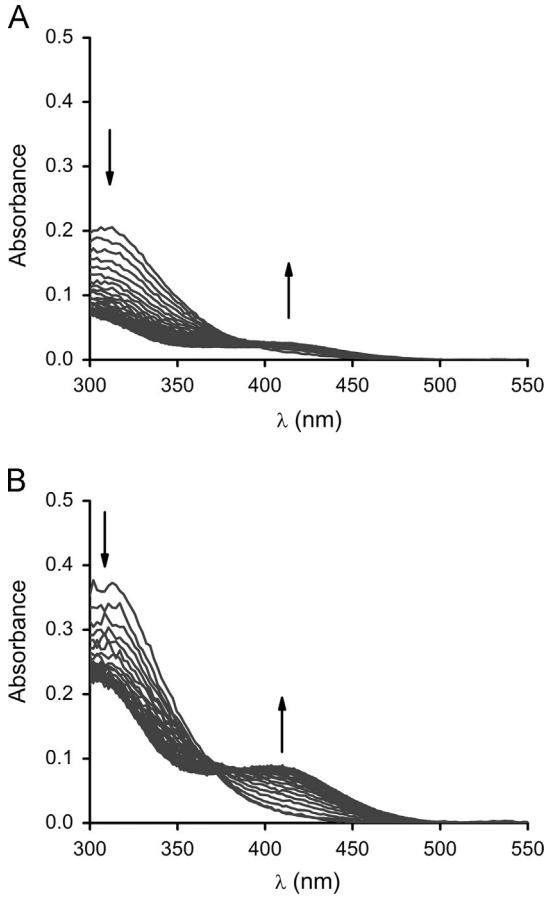

Fig. 8. Reaction between hydrogen sulfide and peroxynitrite in excess. Time-resolved spectra of mixtures obtained after mixing 0.5 mM Na_2S with (A) 0.5 or (B) 2.0 mM peroxynitrite in 0.1 M sodium phosphate with 0.1 mM DTPA, pH 7.4, at 37 °C.

consistent with the analogous reaction of cysteine (10^5–10^8 M^{-1} s^{-1}) [36]. The rate constant of the third step, 3×10^4 M^{-1} s^{-1}, is consistent with HSS^- being more reactive than HS^-. For the simulations, initial concentrations of 2.1 mM hydrogen sulfide and 0.2 mM peroxynitrite were used. These values were chosen to mimic the experimental conditions of Fig. 2 and interrogate the mechanism of the process, and were not intended to reflect biological situations in which the concentrations of hydrogen sulfide and peroxynitrite are estimated to be in the nanomolar range [2,37]. The simulated kinetic profiles for the consumption of peroxynitrite and the formation of the yellow product were remarkably similar to those obtained experimentally (Fig. 9 compared with Fig. 2A). In particular, the formation of the yellow product exhibited a lag phase in the first milliseconds and the k_{obs} obtained from an exponential fit omitting the first 10 ms showed a k_{obs} of 13 s^{-1}, lower than that obtained for peroxynitrite decay, 16 s^{-1}.

Step 1 being the slowest process, the proposed stepwise mechanism is still in agreement with the activation parameters observed previously [6], which suggest an associative character of the reaction and bond interchange.

An alternative sequence that involves the reaction of HSOH (instead of H_2S_2) with peroxynitrite to form the yellow product

cannot explain the observations obtained because peroxynitrite is unlikely to compete with HS^- for HSOH.

H_2S_2 is highly reactive and unstable in water [16]. Its involvement as an intermediate in the formation of the yellow product is conditional to a relatively fast reaction with peroxynitrite. A stock solution of H_2S_2 (prepared in chloroform) was diluted in acetonitrile and mixed with peroxynitrite. The reaction mixture gave an absorbance maximum at ~430 nm and another one at ~610 nm, characteristic for polysulfides (S_3^-) [33] (Fig. 10C). When the buffered solution of the reaction product of peroxynitrite and hydrogen sulfide was diluted with acetonitrile, the absorbance maximum shifted from 408 to 426 nm (Fig. 10A and B), suggesting that the product obtained by mixing H_2S_2 with peroxynitrite is the same as when mixing H_2S with peroxynitrite.

2.6. Product characterization

We addressed the identification of the reaction product by using mass spectrometry. However, the injection of the reaction mixture with normal electron spray ionization led to no product detection. We then performed the reaction in ammonium formate buffer and injected it using cryo-spray ionization at +4 °C. Owing to the high salt concentration we were able to get a weak signal, which we assigned to $[HSNO_2+Na]^+$ (measured *m/z* 101.9424, predicted *m/z* 101.9620) (Fig. 11A and B). A similar peak had been detected before, together with a peak compatible with HSOH [6].

When we diluted the reaction mixture with acetonitrile and sprayed it at −20 °C, much stronger signals were observed. One of the peaks is suggestive of $[2HSNO_2+CH_3CN+NH_4]^+$. Owing to the extremely mild ionization condition and very low temperature, the presence of the solvent in the cluster is quite expected. The observed *m/z* 217.0073 and the isotopic pattern corresponded well to the calculated values (*m/z* 217.0060) (Fig. 11C and D). A higher abundance of m+2 isotope compared to m+1 isotope is characteristic of the presence of sulfur. The most abundant peak in the spectrum remains unassigned, although based on its isotopic pattern it does not seem to contain any sulfur atoms.

Thus, we conclude that $HSNO_2$, or an isomer of it, is at least one of the products formed.

It was proposed that $HSNO_2$ could present three isomeric forms: $HSNO_2$, HSONO, and HS(O)NO [6]. A computational evaluation of the relative energies of these compounds showed that HS(O)NO would not be present as a possible chemical species, because it lies at a very high energy compared to the other isomers. Therefore, we performed UV–Vis absorption prediction calculations for $HSNO_2$ and HSONO, as well as HSSH and HSOH, via linear-response TD-DFT in vacuum as well as hybrid QM–MM real-time TD-DFT calculations in aqueous solution. Moreover, as pK_a values for these species are unknown, protonated and deprotonated species were considered.

An overall analysis of the simulated spectrum (Fig. 12) indicates that the species with nonzero absorption coefficient near 400 nm are $HSNO_2$, either protonated or deprotonated, and HSONO in the protonated state (the latter presenting the higher oscillator strength), supporting the notion that these species can be the yellow product detected experimentally. Moreover, HSSH, HSS^-, and HSOH present null absorption probabilities around 400 nm (See Supplementary Fig. S3).

These results highlight how the conformational exploration and the inclusion of an explicit environment can be crucial in the study of chemical dynamical processes in condensed phases. In the spectra obtained in vacuum and in solution for $HSNO_2$ and HSONO, the absorption probabilities near 400 nm are zero (Supplementary Table S4) in the first case but not in the second one (Fig. 12). This can be interpreted considering that the forbidden character of an electronic transition depends on the symmetry of the system. Therefore, the observed increase in the absorption coefficient near 400 nm in solution versus vacuum simulated spectra can be a consequence of the change in the symmetry caused by the surrounding solvent molecules or due to the fact that the electronic transitions that are forbidden in the optimized geometry of the vacuum structure may not have zero probabilities in all the conformations sampled by the molecular dynamics simulation, hence resulting in a nonzero absorption probability in the average behavior of the system.

Taking together the mass spectrometry detection and the experimental and simulated UV–Vis data, we can conclude that at least one of the products formed is an $HSNO_2$ isomer.

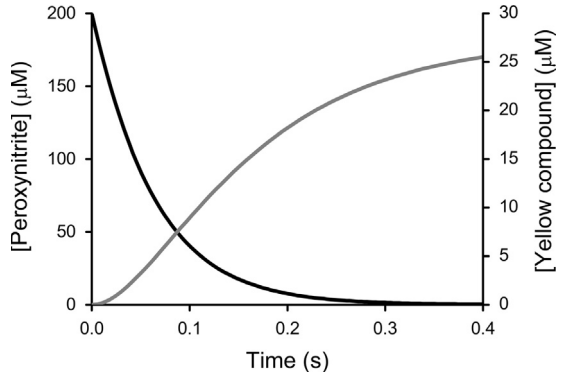

Fig. 9. Computer-assisted simulation of the reaction of hydrogen sulfide with peroxynitrite according to Reactions (1)–(3). The model was set for 2.1 mM Na_2S and 0.2 mM peroxynitrite using the rate constants 6.65 × 10^3, 1 × 10^6, and 3 × 10^4 M^{-1} s^{-1} for k_1, k_2, and k_3, respectively. The black line represents the decay of peroxynitrite, the gray line represents the formation of the yellow product.

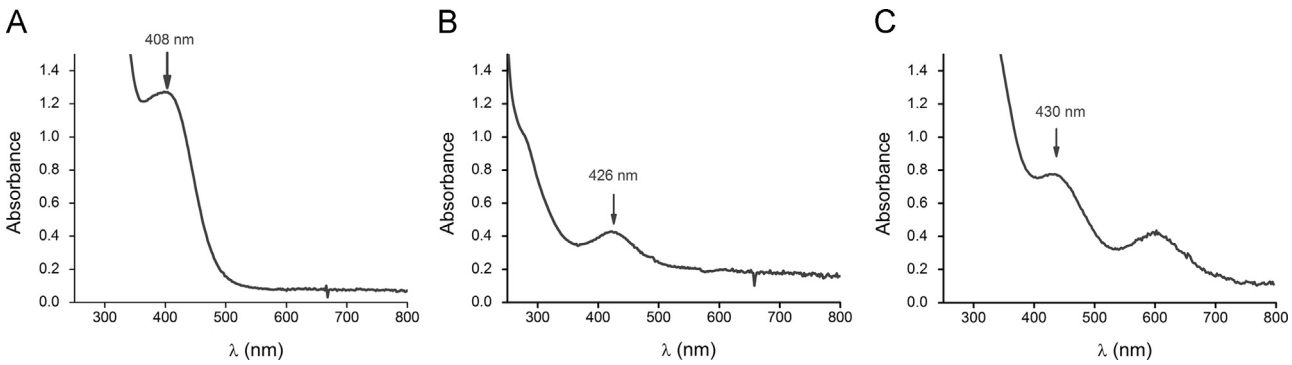

Fig. 10. UV–Vis spectra of the peroxynitrite/sulfide reaction product in organic solvent and its comparison with the peroxynitrite/H_2S_2 reaction product. (A) Peroxynitrite (3.3 mM) was mixed with Na_2S (20 mM) in 500 mM buffer, pH 7.4. (B) The same solution diluted three times in acetonitrile. (C) Peroxynitrite (0.5 mM, final concentration) was mixed with 30 mM H_2S_2 in acetonitrile.

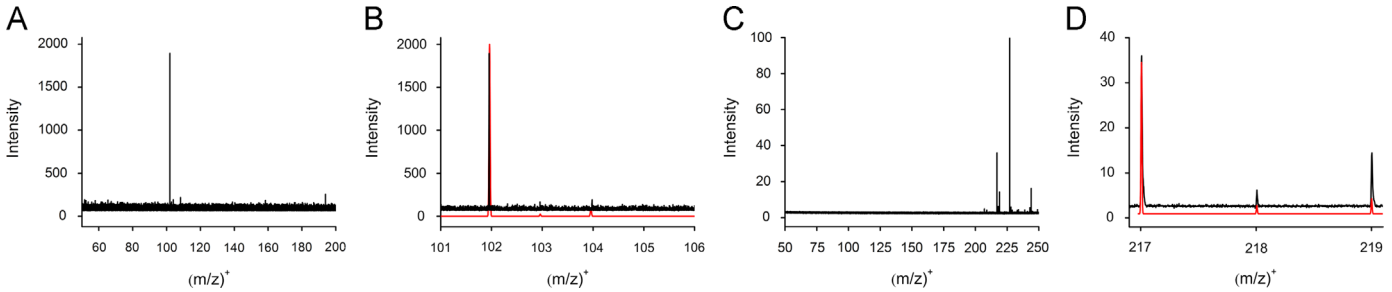

Fig. 11. MS identification of products. (A and B) Peroxynitrite and sulfide were mixed in 20 mM ammonium formate buffer, pH 8.0, and sprayed at +4 °C into ESI–TOF–MS using the cryo-spray technique. (A) Whole spectrum and (B) observed isotopic distribution (black) compared to the predicted distribution (red) for the *m/z* 101.94 peak. (C and D) Reaction mixture prepared in 20 mM ammonium formate was diluted 10 times with acetonitrile and sprayed at −20 °C into ESI–TOF–MS using the cryo-spray technique. (C) Whole-spectrum and (D) observed isotopic distribution (black) compared to the predicted distribution (red) for the *m/z* 217.01 peak.

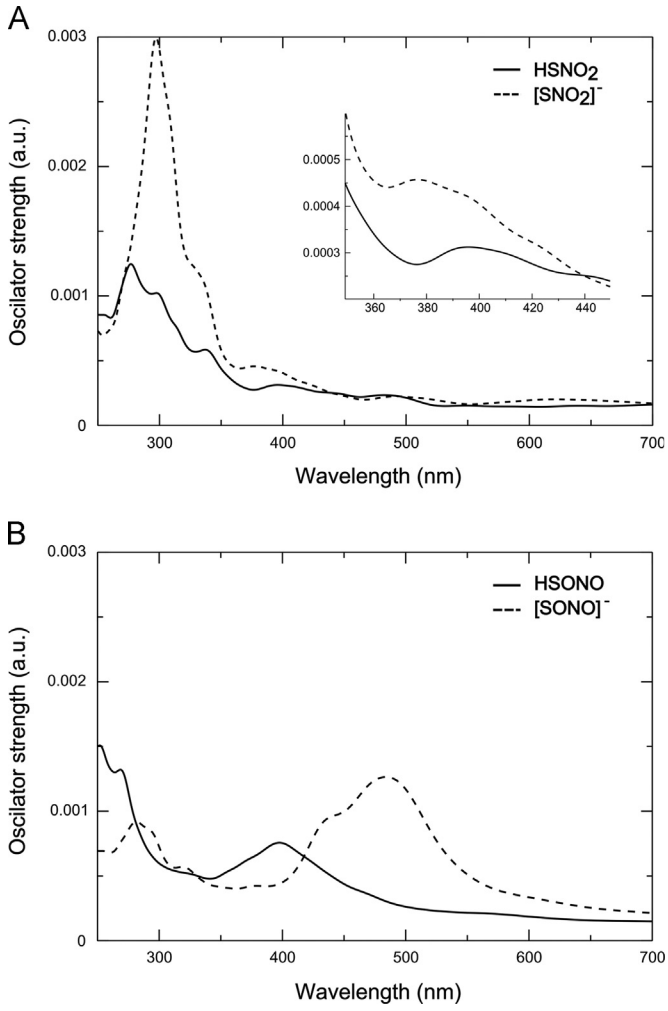

Fig. 12. Predicted UV–Vis absorption spectra for the (A) $HSNO_2$ and (B) HSONO protonated (solid line) and deprotonated (dashed line) forms.

3. Conclusion

The rate constant of the reaction between peroxynitrite and hydrogen sulfide, $(6.65 \pm 0.08) \times 10^3\ M^{-1}\ s^{-1}$ (pH 7.4, 37 °C, 0.05 M sodium phosphate buffer), is affected by the concentration of buffer, explaining the differences observed in earlier reports. According to computational modeling, the reaction is initiated by the nucleophilic attack of hydrosulfide anion on the peroxide group by a typical bimolecular nucleophilic substitution, yielding HSOH and NO_2^-. This mechanism is comparable to that proposed previously for the reaction of thiolates with peroxynitrous acid. However, oxidation of hydrogen sulfide by peroxynitrite yields products different from those expected for thiols, including a yellow product with an absorbance maximum at 408 nm. The kinetic profiles evidence a complex mechanism. The yellow product is not formed in a single step but involves an intermediate, probably HSSH, and its reaction with a second peroxynitrite molecule. Free radicals are unlikely to be involved. Mass spectrometry allowed the detection of a species consistent with $HSNO_2$ and its isomers. Computational predictions of the spectra of the putative compounds involved confirmed that the $HSNO_2$, SNO_2^-, and HSONO isomers could absorb at wavelengths around 400 nm. Thus, at least one of the products formed appears to be $HSNO_2$ or HSONO.

Hydrogen sulfide exerts protective effects on cells exposed to peroxynitrite [6,38]. Nevertheless, according to the second-order rate constant of $6.65 \times 10^3\ M^{-1}\ s^{-1}$ together with the relatively low concentrations of hydrogen sulfide estimated in vivo (~15 nM) [2], the protective effects are unlikely to be explained by direct scavenging of peroxynitrite by hydrogen sulfide. Possible explanations are speculative at this stage and warrant further research into the interplay between these captivating molecules.

Acknowledgments

We thank Dr. Matías N. Möller (Universidad de la República, Uruguay) and Dr. Damián A. Scherlis (Universidad de Buenos Aires and CONICET, Argentina) for helpful discussions. This work was financed by grants from the CSIC, Universidad de la República, and L'Oréal–UNESCO, Uruguay (to B.A.). E.C. was partially supported by fellowships from the Agencia Nacional de Investigación e Innovación and PEDECIBA, Uruguay. M.R.F. and R.W. acknowledge support from an intramural grant from the FAU Erlangen–Nuremberg within Emerging Field Initiative (MRIC). The authors are grateful to Professor Ivana Ivanovic-Burmazovic for the use of cryo-spray MS.

Appendix A. Supporting information

Supplementary data associated with this article can be found in the online version at http://dx.doi.org/10.1016/j.freeradbiomed.2014.12.017.

References

[1] Kabil, O.; Banerjee, R. Redox biochemistry of hydrogen sulfide. *J. Biol. Chem.* **285:**21903–21907; 2010.
[2] Furne, J.; Saeed, A.; Levitt, M. D. Whole tissue hydrogen sulfide concentrations are orders of magnitude lower than presently accepted values. *Am. J. Physiol. Regul. Integr. Comp. Physiol* **295:**R1479–R1485; 2008.
[3] Abe, K.; Kimura, H. The possible role of hydrogen sulfide as an endogenous neuromodulator. *J. Neurosci.* **16:**1066–1071; 1996.

[4] Zhao, W.; Zhang, J.; Lu, Y.; Wang, R. The vasorelaxant effect of H(2)S as a novel endogenous gaseous K(ATP) channel opener. *EMBO J.* **20:**6008–6016; 2001.

[5] Carballal, S.; Trujillo, M.; Cuevasanta, E.; Bartesaghi, S.; Möller, M. N.; Folkes, L. K.; García-Bereguiaín, M. A.; Gutiérrez-Merino, C.; Wardman, P.; Denicola, A.; Radi, R.; Alvarez, B. Reactivity of hydrogen sulfide with peroxynitrite and other oxidants of biological interest. *Free Radic. Biol. Med.* **50:**196–205; 2011.

[6] Filipovic, M. R.; Miljkovic, J.; Allgäuer, A.; Chaurio, R.; Shubina, T.; Herrmann, M.; Ivanovic-Burmazovic, I. Biochemical insight into physiological effects of H_2S: reaction with peroxynitrite and formation of a new nitric oxide donor, sulfinyl nitrite. *Biochem. J.* **441:**609–621; 2012.

[7] Radi, R.; Beckman, J. S.; Bush, K. M.; Freeman, B. A. Peroxynitrite oxidation of sulfhydryls: the cytotoxic potential of superoxide and nitric oxide. *J. Biol. Chem.* **266:**4244–4250; 1991.

[8] Trujillo, M.; Radi, R. Peroxynitrite reaction with the reduced and the oxidized forms of lipoic acid: new insights into the reaction of peroxynitrite with thiols. *Arch. Biochem. Biophys.* **397:**91–98; 2002.

[9] Carballal, S.; Radi, R.; Kirk, M. C.; Barnes, S.; Freeman, B. A.; Alvarez, B. Sulfenic acid formation in human serum albumin by hydrogen peroxide and peroxynitrite. *Biochemistry* **42:**9906–9914; 2003.

[10] Trujillo, M.; Clippe, A.; Manta, B.; Ferrer-Sueta, G.; Smeets, A.; Declercq, J. P.; Knoops, B.; Radi, R. Pre-steady state kinetic characterization of human peroxiredoxin 5: taking advantage of Trp84 fluorescence increase upon oxidation. *Arch. Biochem. Biophys.* **467:**95–106; 2007.

[11] Ferrer-Sueta, G.; Manta, B.; Botti, H.; Radi, R.; Trujillo, M.; Denicola, A. Factors affecting protein thiol reactivity and specificity in peroxide reduction. *Chem. Res. Toxicol.* **24:**434–450; 2011.

[12] Zeida, A.; González Lebrero, M. C.; Radi, R.; Trujillo, M.; Estrin, D. A. Mechanism of cysteine oxidation by peroxynitrite: an integrated experimental and theoretical study. *Arch. Biochem. Biophys.* **539:**81–86; 2013.

[13] Peshenko, I. V.; Shichi, H. Oxidation of active center cysteine of bovine 1-Cys peroxiredoxin to the cysteine sulfenic acid form by peroxide and peroxynitrite. *Free Radic. Biol. Med.* **31:**292–303; 2001.

[14] Saha, A.; Goldstein, S.; Cabelli, D.; Czapski, G. Determination of optimal conditions for synthesis of peroxynitrite by mixing acidified hydrogen peroxide with nitrite. *Free Radic. Biol. Med.* **24:**653–659; 1998.

[15] Hughes, M. N.; Nicklin, H. G. The chemistry of pernitrites. Part I. Kinetics of decomposition of pernitrous acid. *J. Chem. Soc. A* :450–452; 1968.

[16] Brauer, G. *Handbook of Preparative Inorganic Chemistry*. 2nd ed.. San Diego: Academic Press; 1963.

[17] Gaussian 03. *Wallingford (CT)*. Gaussian, Inc; 2004.

[18] Godbout, N.; Salahub, D. R.; Andzelm, J.; Wimmer, E. Optimization of Gaussian-type basis sets for local spin density functional calculations. Part I. Boron through neon, optimization technique and validation. *Can. J. Chem.* **70:**560–571; 1992.

[19] Nitsche, M. A.; Ferreria, M.; Mocskos, E. E.; González Lebrero, M. C. GPU accelerated implementation of density functional theory for hybrid QM/MM simulations. *J. Chem. Theory Comput.* **10:**959–967; 2014.

[20] Morzan, U. N.; Ramírez, F. F.; Oviedo, M. B.; Sánchez, C. G.; Scherlis, D. A.; Gonzalez-Lebrero, M. C. Electron dynamics in complex environments with real-time time dependent density functional theory in a QM–MM framework. *J. Chem. Phys.* **140:**164105; 2014.

[21] Mendes, P. GEPASI: a software package for modelling the dynamics, steady states and control of biochemical and other systems. *Comput. Appl. Biosci.* **9:**563–571; 1993.

[22] Hughes, M. N.; Centelles, M. N.; Moore, K. P. Making and working with hydrogen sulfide. The chemistry and generation of hydrogen sulfide in vitro and its measurement in vivo: a review. *Free Radic. Biol. Med.* **47:**1346–1353; 2009.

[23] Kissner, R.; Nauser, T.; Bugnon, P.; Lye, P. G.; Koppenol, W. H. Formation and properties of peroxynitrite as studied by laser flash photolysis, high-pressure stopped-flow technique, and pulse radiolysis. *Chem. Res. Toxicol.* **10:**1285–1292; 1997.

[24] Squadrito, G. L.; Pryor, W. A. Mapping the reaction of peroxynitrite with CO_2: energetics, reactive species, and biological implications. *Chem. Res. Toxicol.* **15:**885–895; 2002.

[25] Cotton, F.; Wilkinson, G. *Advanced Inorganic Chemistry*. New York: Wiley Intersci.; 1988.

[26] Jursic, B. S.; Klasinc, L.; Pecur, S.; Pryor, W. A. On the mechanism of HOONO to HONO2 conversion. *Nitric Oxide* **1:**494–501; 1997.

[27] Dixon, D. A.; Feller, D.; Zhan, C. -G.; Francisco, J. S. Decomposition pathways of peroxynitrous acid: gas-phase and solution energetics. *J. Phys. Chem. A* **106:**3191–3196; 2002.

[28] Gonzalez Lebrero, M. C.; Perissinotti, L. L.; Estrin, D. A. Solvent effects on peroxynitrite structure and properties from QM/MM simulations. *J. Phys. Chem. A* **109:**9598–9604; 2005.

[29] Zeida, A.; Babbush, R.; Gonzalez-Lebrero, M. C.; Trujillo, M.; Radi, R.; Estrin, D. A. Molecular basis of the mechanism of thiol oxidation by hydrogen peroxide in aqueous solution: challenging the SN2 paradigm. *Chem. Res. Toxicol.* **25:**741–746; 2012.

[30] Denicola, A.; Freeman, B. A.; Trujillo, M.; Radi, R. Peroxynitrite reaction with carbon dioxide/bicarbonate: kinetics and influence on peroxynitrite-mediated oxidations. *Arch. Biochem. Biophys.* **333:**49–58; 1996.

[31] Denicola, A.; Souza, J. M.; Gatti, R. M.; Augusto, O.; Radi, R. Desferrioxamine inhibition of the hydroxyl radical-like reactivity of peroxynitrite: role of the hydroxamic groups. *Free Radic. Biol. Med.* **19:**11–19; 1995.

[32] Miljkovic, J. L.; Kenkel, I.; Ivanović-Burmazović, I.; Filipovic, M. R. Generation of HNO and HSNO from nitrite by heme-iron-catalyzed metabolism with H_2S. *Angew. Chem. Int. Ed. Engl.* **52:**12061–12064; 2013.

[33] Wedmann, R.; Bertlein, S.; Macinkovic, I.; Böltz, S.; Miljkovic, J. L.; Muñoz, L. E.; Herrmann, M.; Filipovic, M. R. Working with H_2S: facts and apparent artifacts. *Nitric Oxide* **41:**85–96; 2014.

[34] Filipovic, M. R.; Miljkovic, J. L.; Nauser, T.; Royzen, M.; Klos, K.; Shubina, T.; Koppenol, W. H.; Lippard, S. J.; Ivanović-Burmazović, I. Chemical characterization of the smallest S-nitrosothiol, HSNO; cellular cross-talk of H_2S and S-nitrosothiols. *J. Am. Chem. Soc.* **134:**12016–12027; 2012.

[35] Kotronarou, A.; Hoffmann, M. R. Peroxymonosulfate: an alternative to hydrogen peroxide for the control of hydrogen sulfide. *Res. J. Water Pollut. Control Fed* **63:**965–970; 1991.

[36] Ashby, M. T.; Nagy, P. On the kinetics and mechanism of the reaction of cysteine and hydrogen peroxide in aqueous solution. *J. Pharm. Sci.* **95:**15–18; 2006.

[37] Ferrer-Sueta, G.; Radi, R. Chemical biology of peroxynitrite: kinetics, diffusion, and radicals. *ACS Chem. Biol.* **4:**161–177; 2009.

[38] Whiteman, M.; Armstrong, J. S.; Chu, S. H.; Jia-Ling, S.; Wong, B. S.; Cheung, N. S.; Halliwell, B.; Moore, P. K. The novel neuromodulator hydrogen sulfide: an endogenous peroxynitrite scavenger? *J. Neurochem.* **90:**765–768; 2004.